Supplementary Materials

Injectable Multi-Component Hydrogels for the Treatment of Ascites caused by Hepatocellular Carcinoma via Anti-tumor and Reduction of Ascites Generation

Yuqin Yang [a, †], Jinchai Qi[b, †], Yingqi Lang [b †], Meiling Wu [a], Yixiao Gu[a], Xinyue Lu [a], Minshu Wang [a], Qibiao, Wu [c], Fuhao Chu [b, *], Mengru Cai [a, *], Keyang Xu [c, *]

[a] Institute of Basic Theory for Chinese Medicine, China Academy of Chinese Medical Sciences, Beijing 100700, China

[b] Beijing University of Chinese Medicine, Beijing 102488, China

[c] Faculty of Chinese Medicine, and State Key Laboratory of Mechanism and Quality of Chinese Medicine, Macau University of Science and Technology, Macau 999078, China.

[†] These authors contributed equally to this work

* Correspondence author

E-mail address: chufhao@163.com (F. Chu); cmr199711@163.com (M. Cai); kyxu@must.edu.mo (K. Xu)

Phone: 010-64089011, (853)8897-2261; *Fax:* 010-64289002, (853)2882-5123

1. Methods

1.1 Sample Preparation

Genkwa Flos (50 g) was packed in a nonwoven bag (5 cm × 7 cm, pore diameter <30 μm) and transferred into a 1000-mL round-bottom flask. Water (500 mL) was added and then heated for 1 h under reflux. The filtrate of the *Genkwa Flos* solution was concentrated using a Rotavapor R-215 rotary evaporator (BUCHI, Flawil, Switzerland) to a volume of 50 mL. The solution was then transferred to a separatory funnel and extracted with 50 mL of ethyl acetate three times. The ethylacetate extract was lyophilized using a Martin Christ Beta 2–8 LD plus freeze dryer (Osterode, Germany). The resulting *Genkwa Flos* extract powder (25 mg) was combined with 20

mg of glycyrrhizic acid in a 100-mL round-bottom flask. Water (10 mL) was added, and then extracted with reflux for 1 h to obtain a uniform solution. Then, the solution was cooled at room temperature to obtain a homogeneous and stable hydrogel (GK-GA).

1.2 Scanning Electron Microscopy Test

Scanning electron microscope (SEM) images were recorded on a ZEISS-SUPRA55 SEM spectrometer at 10 kV. 2.5 μL of the solutions were dropped on the silicon by a pipette, respectively. Then the samples were dried at room temperature for 4 h. Then the images were recorded at 10 kV. Prior to observation, the xerogel samples were sputter-coated with a thin layer of gold.

1.3 Network Pharmacological Analysis

Collection of Candidate Ingredients and Targets for GK-GA

The potential GK-GA candidate ingredients were obtained from previously reported [1]. and the candidate ingredients-related protein targets were collected from Swiss Target Prediction (http://www.swisstargetprediction.ch/).

Collection of Potential Targets for Malignant Ascites

Firstly, we used “malignant ascites” as a search term in the GeneCards database (https://www.genecards.org/) and retrieved a range of disease targets related to malignant ascites. Next, we identified the intersection between disease targets and the targets of candidate ingredients of GK-GA.

Network Construction and Analysis

We constructed an interaction network of candidate ingredients and predictive targets of GK-GA for the treatment of malignant ascites and visualized the interaction network using Cytoscape software (version 3.7.2). Cytoscape's Network analyzer analysis of degree, betweenness centrality, and closeness centrality was used to measure the topological importance of nodes in a network.

1.4 Molecular Dynamics Simulations

The initial configurations of this system with 10 Glycyrrhizic acid (GA), 10 Genkwanin (GKW) and 3000 water molecules were constructed through the software of packmol [2], the molecules were randomly inserted into a cubic simulation box. The force field GAFF [3] was employed to describe the GA and GKW molecules. The molecular force field consists nonbonded and bonded interaction. The nonbonded interaction contains van deer Waals (vdW) and electrostatic interaction, which is described by Equation 1 and Equation 2, respectively.

$$E_{LJ}\left(r_{ij}\right)=4\varepsilon_{ij}\left(\left(\frac{\varepsilon_{ij}}{r_{ij}}\right)^{12}-\left(\frac{\varepsilon_{ij}}{r_{ij}}\right)^{6}\right) \tag{1}$$

$$E_{c}\left(r_{ij}\right)=\frac{q_{i}q_{j}}{4\pi\varepsilon_{o}\varepsilon_{r}r_{ij}} \tag{2}$$

The cutoff distance of vdW and electronic interaction was set to 1.2 nm, and the particle mesh Ewald (PME) method was employed to calculate long-range electrostatic interactions.

For this simulation, an energy minimization was firstly employed to relax the simulation box. Then, a canonical (NVT) ensemble where the temperature is set to 298.15 K with a 2.0 fs time step is employed to optimize the simulation box. The Nose-Hoover thermostat is used to maintain the temperature. The NVT optimization time was set to 10.0 ns, which is enough long to obtain a stable box size. Following the NVT simulation, an isothermal-isobaric (NPT) ensemble with 100.0 ns was performed to furtherly optimize the simulation box, the time step was kept at 2.0 fs. The optimized simulation boxes were shown in Figure 1. In all the MD simulations, the motion of atoms was described by the classical Newton's equation, which was solved using the velocity-Verlet algorithm. All simulations were performed using the GROMACS 2020.7 package [4]. The Visualization of structure was performed by VMD software [5].

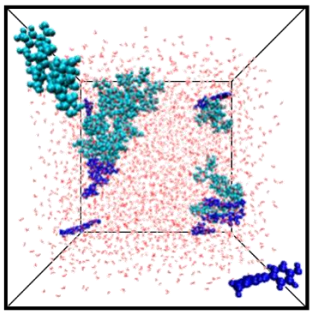

Figure 1. The initial configurations of Glycyrrhizic acid (cyan color) and Genkwanin (blue color) in the water (red color).

1.5 *In vitro* Cytotoxicity Assay of GK, GA, and GK-GA in Hepatoma 22

Firstly, Hepatoma 22 cells were incubated into 96-well plate. After 24 h incubation, different concentrations of GK, GA, and GK-GA were added respectively. Afterwards, CCK-8 was added after 24 h of culture, then the absorbance was measured after 2 h at 450 nm.

1.6 Detection of Apoptosis using Annexin V-FITC/PI Staining

The cell apoptosis assay was performed with the Annexin V-FITC/PI apoptosis detection kit instructions (Solarbio, Beijing, China). Briefly, H22 cells in logarithmic growth phase were seeded in 6-well plates (4.8×10^4 cells/well). After incubation for 24 h at 37℃ in a humidified atmosphere with 5% CO_2, certain concentrations of GK-GA (0.07813, 0.15625, 0.3125 $mg \cdot mL^{-1}$) was added to each well, and the plate was incubated for further 24 h. Then, H22 cells was collected respectively and washed twice with cold PBS (4°C) and centrifuged at 2400 rpm for 10 min. After that, the supernatant was discarded and the resulting pellet was resuspended in 100 μL binding buffer, which contained 5 μL Annexin V-FITC and 5 μL PI. After incubation at room temperature for 10 min in the dark, the cells were added to another 100 μL binding buffer, the samples were analyzed by flow cytometry (BD FACSCelesta, New Jersey, USA). The experiment was performed independently in triplicate.

1.7 RNA sequencing (RNA-seq) analysis

The H22 ascites cells of the model and GK-GA groups were collected and the total RNA was extracted from three biological replicates using TRIZOL reagent according to the manufacturer's instructions (Invitrogen, USA). The genomic DNA was removed from the prepared samples using DNase I (Takara, Japan). RNA quality was assessed using the 2100 Bioanalyser (Agilent Technologies, SanDiego, CA, USA). Samples with RNA integrity numbers (RINs) > 9.4 and with 260/280 nm absorbance ratios from 1.9 to 2.1 were used for the construction of RNA-seq libraries. Library preparation and sequencing were performed by Majorbio Biotech (Shanghai, China) on an Illumina NovaSeq 6000 sequencer. The data were analyzed on the free online Majorbio I-Sanger Cloud Platform (www.i-sanger.com).

1.8 The Real-Time Quantitative Polymerase Chain Reaction (qPCR)

Total RNA was extracted from the H22 ascites cells using TRIZOL reagent according to the manufacturer's instructions (Invitrogen, USA) and was reverse-transcribed into cDNA using First Strand cDNA Synthesis Kit With gDNA Eraser (11119ES60, Yeasen, Shanghai, China). Real-time qPCR was performed on an Applied Biosystems FS384 real-time PCR system using the SYBR Premix Ex Taq (Tli RNase H Plus) (11203ES03, Yeasen, Shanghai, China). Primers for the target genes were synthesized by Majorbio Biotech (Shanghai, China). Primer sequences for genes were listed in Table 1. Primer specificity was confirmed by a dissociation curve using the 7500 system SDS software. Glyceraldehyde 3-phosphate dehydrogenase (GAPDH) was used as the internal control.

1.9 Western Blotting Assay

The H22 ascites cells were lysed in ice-cold radio-immunoprecipitation assay (RIPA) buffer containing protease and phosphatase inhibitors (Phenylmethylsulfonyl fluoride, PMSF) (Servicebio, Wuhan, China). Total protein was measured by the

bicinchoninic acid protein assay (BCA, Servicebio, Wuhan, China) method. Antibodies against ERK1 and SRC were obtained from Servicebio Biotechnology Co. LTD (Wuhan, China). The normalization control was anti-β-actin (Servicebio, Beijing, China). Immune complexes were detected using immobilon western chemiluminescent HRP substrate (Servicebio, Beijing, China). Bands were quantified by densitometry using AlphaEaseFC software (AlphaInnotech, San Leandro, CA).

1.10 Non-targeted Metabolomics of the Model and the GK-GA groups

1.10.1 Metabolites Extraction

The samples (100 μL) were placed in the EP tubes and resuspended with prechilled 80% methanol by well vortex. Then the samples were incubated on ice for 5 min and centrifuged at 15,000 g, 4°C for 20 min. Some of supernatant was diluted to final concentration containing 53% methanol by LC-MS grade water. Samples were subsequently transferred to a fresh Eppendorf tube and then were centrifuged at 15000 g, 4°C for 20 min. Finally, the supernatant was injected into the LC MS/MS system analysis [6, 7].

1.10.2 UHPLC-MS/MS Analysis

UHPLC-MS/MS analyses were performed using a Thermo Syncronis C_{18} (2.1 mm × 100 mm, 1.7 μm) UHPLC system (Thermo Fisher, Germany) coupled with an Orbitrap Q Exactive TM series mass spectrometer (Thermo Fisher， Germany) in Scale Co., Ltd. (Beijing, China). Samples were injected onto a Hypesil Gold column (2.1 mm × 100 mm, 1.7 μm) using a 18-min linear gradient at a flow rate of 0.2 mL/min. The eluents A and B were 0.1% FA in water and acetonitile respectively. The solvent gradient was set as follows: 0~1 min, 95% A; 1~5 min, 95%~40% A; 5~8 min, 40%~0% A; 8~11 min, 0% A; 11~14 min, 0%~40% A; 11~15 min, 40%~95% A, 15~18 min, 95% A. Q ExactiveTM series mass spectrometer was operated in positive/negative polarity

mode or positive/negative auto-switching mode with spray voltage of 3.2 kV, capillary temperature of 320°C, sheath gas flow rate of 40 arb and aux gas flow rate of 10 arb.

1.10.3 Data processing and metabolite identification

The raw data files generated by UHPLC-MS/MS were processed using the TraceFinder3.2.0 (Thermo Fisher) to perform peak alignment, peak picking, and quantitation for each metabolite. The main parameters were set as follows: retention time tolerance, 0.2 minutes; actual mass tolerance, 5ppm; signal/noise ratio, 3; and minimum intensity, et al. After that, peak intensities were normalized to the total spectral intensity. And then peaks were matched with the mzCloud (https://www.mzcloud.org/) and self-built database to obtain the accurate qualitative and relative quantitative results. The statistical analyses were performed using the statistical software R (R version R-3.4.3), Python (Python 2.7.6 version) and CentOS (CentOS release 6.6). When data were not normally distributed, normal transformations were attempted using of area normalization method.

1.10.4 Data Analysis

These metabolites were annotated using the KEGG database (https://www.genome.jp/kegg/pathway.html), HMDB database (https://hmdb.ca/metabolites) and LIPID Maps database (http://www.lipidmaps.org/). Principal components analysis (PCA) and Partial least squares discriminant analysis (PLS-DA) were performed at metaX [8] (a flexible and comprehensive software for processing metabolomics data). We applied univariate analysis (t-test) to calculate the statistical significance (P-value). The metabolites with VIP > 1 and P-value< 0.05 and fold change≥2 or FC≤0.5 were considered to be differential metabolites. Volcano plots were used to filter metabolites of interest which based on log2 (Fold Change) and -log10 (p-value) of metabolites by ggplot2 in R language.

1.11 Steroid-targeted metabolomics of Model and GK-GA

According to the result of untargeted metabolome, the verification of steroids targeted metabolomic was carried out. Steroids contents were detected by MetWare (http://www.metware.cn/) based on the AB Sciex QTRAP 6500 LC-MS/MS platform.

2. Results

Table S1. Information on the constituents in GK-GA hydrogel

Number	Name	Structure	Number	Name	Structure
1	adenine	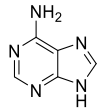	**2**	trigonelline	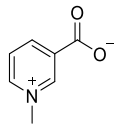
3	phenylacetaldehyde	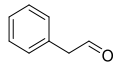	**4**	L-leucine	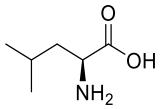
5	L-phenylalanine	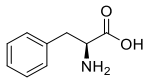	**6**	guanosine	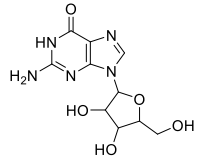
7	adenosine	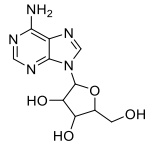	**8**	chlorogenic acids	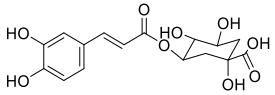
9	neochlorogenic acid	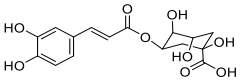	**10**	cryptochlorogenic acid	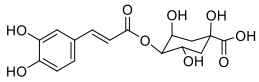
11	scopolin	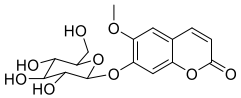	**12**	7-hydroxycoumarin	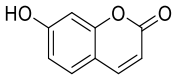
13	schaftoside	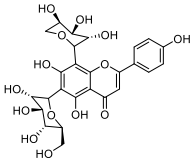	**14**	diosmetin	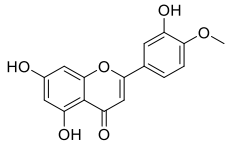

Continue **Table S1**

Number	Name	Structure	Number	Name	Structure
15	luteoloside	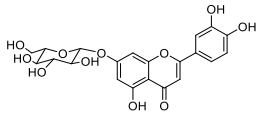	**16**	astragalin	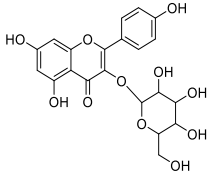
17	3-O-β-D-glucoside-kaempferol	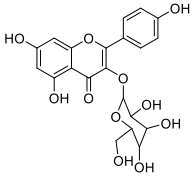	**18**	vitexin	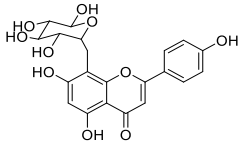
19	kaempferol-3-O-glucorhamnoside	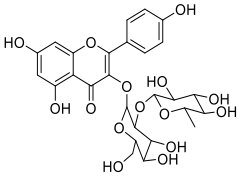	**20**	α-cyperone	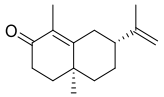
21	genistin	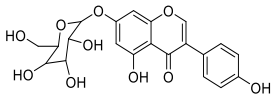	**22**	apigenin	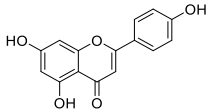
23	genkwanin	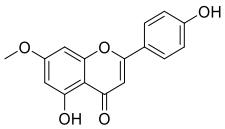	**24**	oroxylin	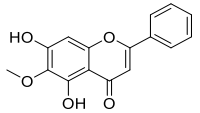

Continue **Table S1**

Number	Name	Structure	Number	Name	Structure
25	wogonin	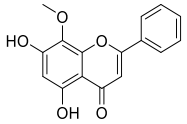	**26**	calycosin	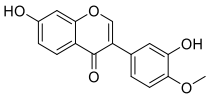
27	Tiliroside	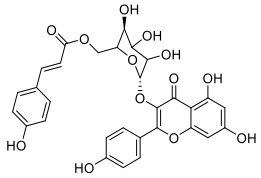	**28**	kaempferol	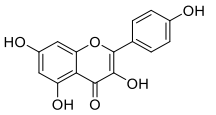
29	scutellarein	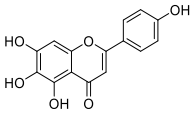	**30**	wogonoside	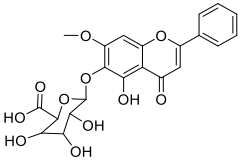
31	sakuranetin	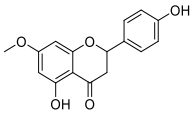	**32**	hydroxygenkwanin	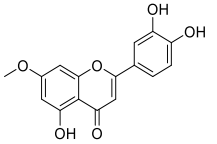
33	hispidulin	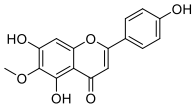	**34**	3′, 4′-dihydroxy-3, 7-dimethoxyflavone	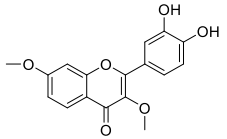
35	5, 7-dihydroxy-6, 8-dimethoxyflavone	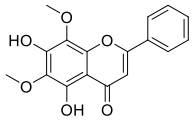	**36**	yuanhuafine	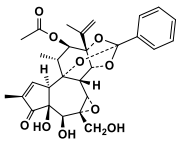

Continue **Table S1**

Number	Name	Structure	Number	Name	Structure
37	yuanhuatine	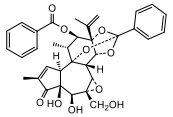	**38**	genkwadaphnine	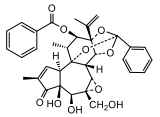
39	yuanhuacine	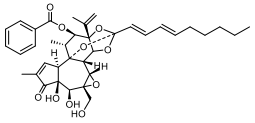	**40**	Yuanhuapine	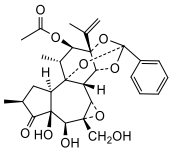
41	7-ketositosterol	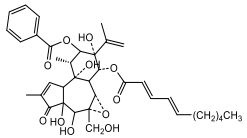	**42**	9-Hydroxyglabratolide	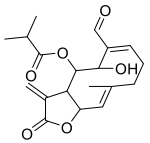
43	Gentiacaulein	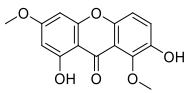	**44**	yuanhuadine	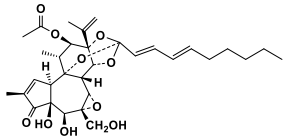
45	luteolin	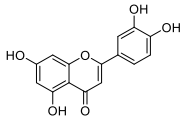	**46**	quercetin	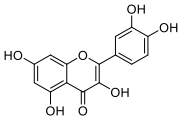
47	yuenkanin	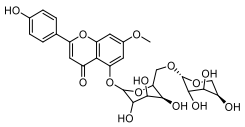	**48**	Glycyrrhizic acid	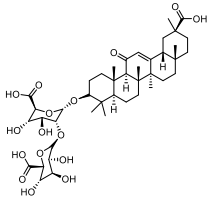

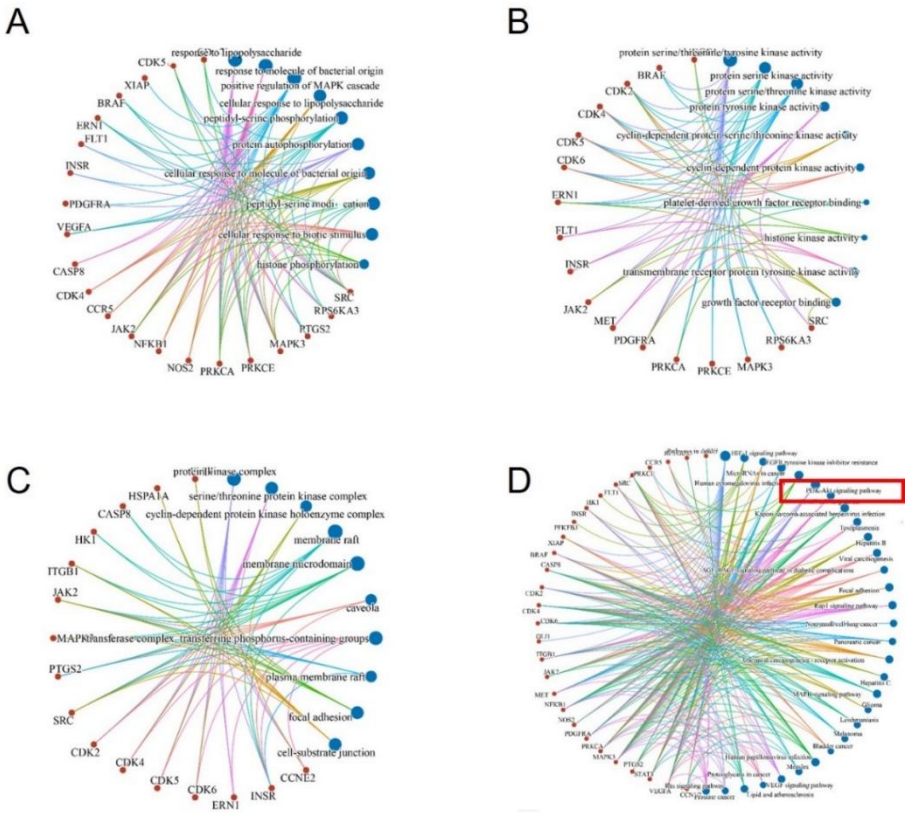

Fig. S1. GO & KEGG enrichment analysis. A Gene ontology (GO) enrichment analysis on Biological Process (BP). **B** Gene ontology (GO) enrichment analysis on Cellular Component (CC). **C** Gene ontology (GO) enrichment analysis on Molecular Function (MF). **D** KEGG enrichment analysis.

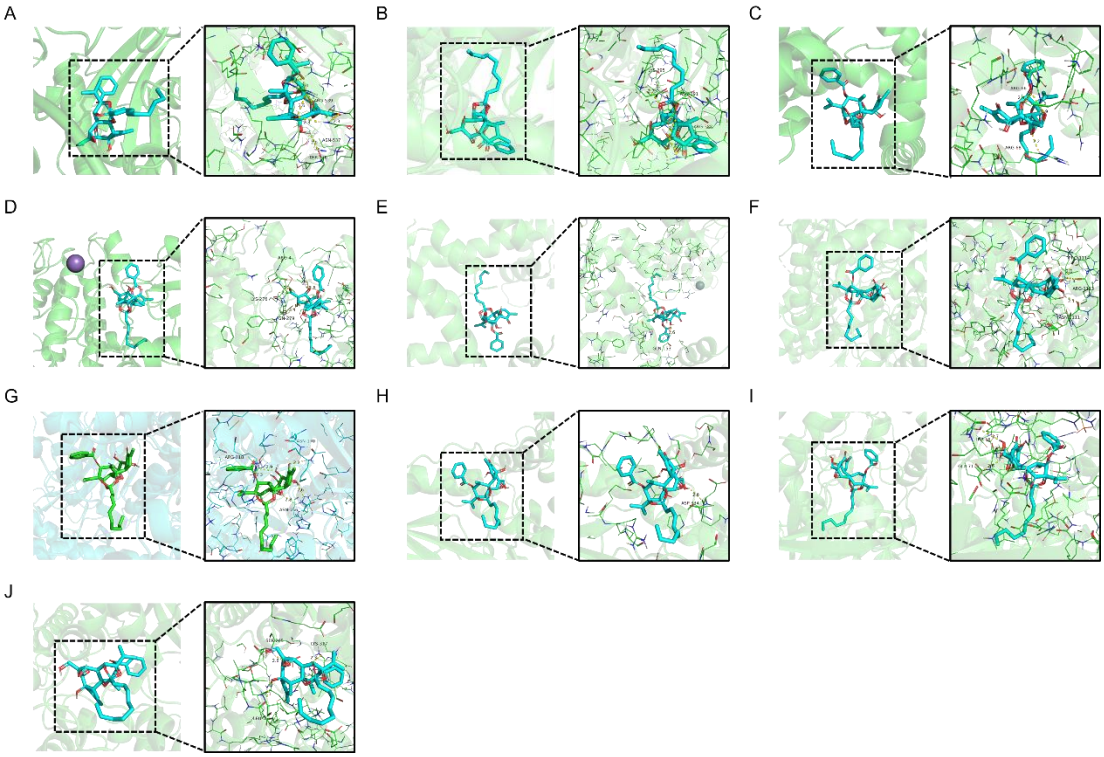

Fig. S2 Molecular docking of Yuanhuacine with HK1 **A** SRC **B**, BCL2 **C**, AKT1 **D**, SEC31A **E**, JAK2 **F,** PI3K **G**, STAT3 **H**, ATF2 **I**, and MAPK3 **J**.

HK1, BCL2, SEC31A, ATF2

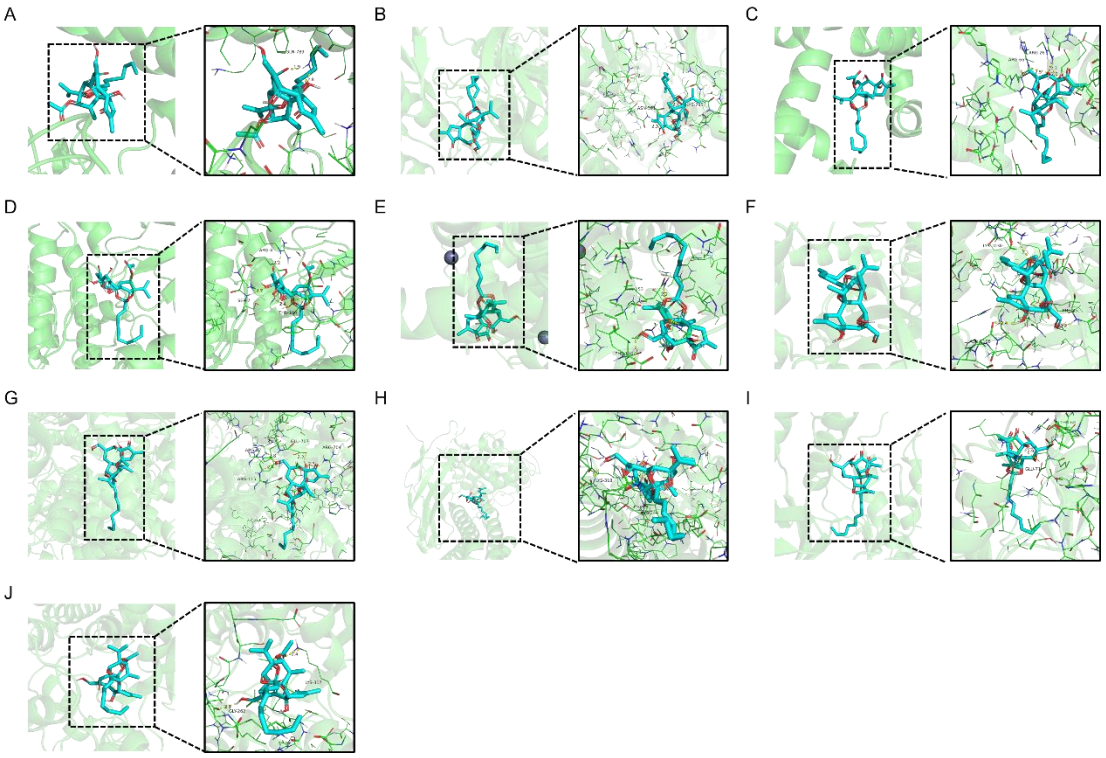

Fig. S3 Molecular docking of Yuanhuadine with HK1 **A**, SRC **B**, BCL2 **C**, AKT1 **D**, SEC31A **E**, JAK2 **F**, PI3K **G**, STAT3 **H**, ATF2 **I**, and MAPK3 **J**.

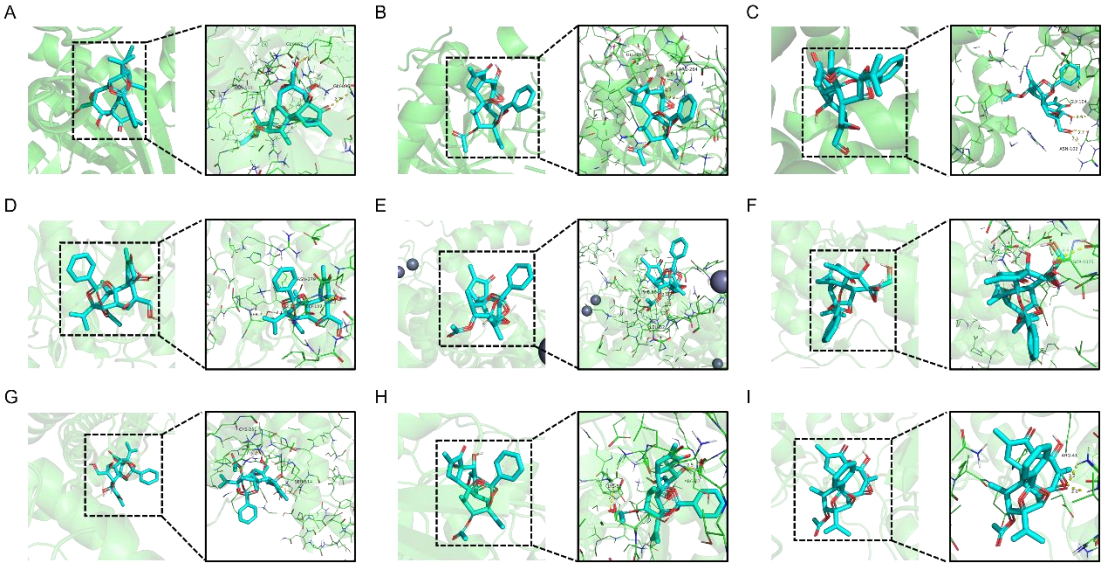

Fig. S4 Molecular docking of Yuanhuafine with HK1 **A**, SRC **B**, BCL2 **C**, AKT1 **D**, SEC31A **E**, JAK2 **F**, STAT3 **G**, ATF2 **H**, and MAPK3 **I**.

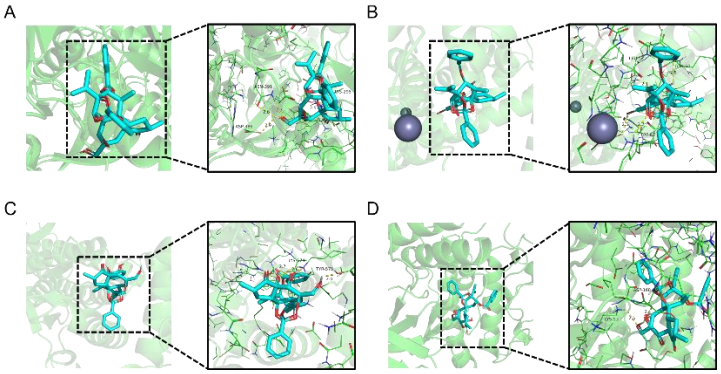

Fig. S5 Molecular docking of Yuanhuatine with SRC **A**, SEC31A **B**, STAT3 **C**, and ATF2 **D**.

Table S2. 43 kinds of steroid hormones

Number	Name	CAS	Number	Name	CAS
1	Testosterone	58-22-0	**2**	Dihydrotestosterone	521-18-6
3	Androsterone	53-41-8	**4**	5β-Androsterone	53-42-9
5	dehydroepiandrosterone	53-43-0	**6**	Androstenedione	63-05-8
7	Androstanedione	846-46-8	**8**	11-Hydroxyandrosterone	57-61-4
9	11-Ketoetiocholanolone	739-27-5	**10**	Cortisol	50-23-7
11	11-Dehydrocorticosterone	72-23-1	**12**	Deoxycorticosterone	64-85-7
13	Corticosterone	50-22-6	**14**	Cortexolone	152-58-9
15	Aldosterone	52-39-1	**16**	Cortisone	53-06-5
17	17β-Estradiol	50-28-2	**18**	17a-Estradiol	57-91-0
19	Estrone	53-16-7	**20**	17α-Ethinylestradiol	57-63-6
21	16α-Hydroxy Estrone	566-76-7	**22**	2-Methoxy Estrone	362-08-3
23	4-Methoxy Estrone	58562-33-7	**24**	2-Hydroxy-Estrone	362-06-1
25	Pregnenolone	145-13-1	**26**	17α-Hydroxypregnenolone	387-79-1
27	5alpha-Pregnane-3,20-dione	566-65-4	**28**	Progesterone	57-83-0
29	17a-Hydroxyprogesterone	68-96-2	**30**	Pregnanediol	80-92-2

Continue Table S2. 43 kinds of steroid hormones

Number	Name	CAS	Number	Name	CAS
31	24-Hydroxycholesterol	474-73-7	**32**	7α,25-Dihydroxycholesterol	64907-22-8
33	Cholesterol	57-88-5	**34**	24,25-Dihydrolanosterol	79-62-9
35	25-Hydroxycholesterol	2140-46-7	**36**	Desmosterol	313-04-2
37	Lathosterol	80-99-9	**38**	7-Hydroxy-cholesten-3-one	3862-25-7
39	20α-Hydroxycholesterol	516-72-3	**40**	7-Ketocholesterol	566-28-9
41	7a,27-Dihydroxycholesterol	4725-24-0	**42**	*β*-Sitosterol	83-46-5
43	Vitamin D3	67-97-0			

Reference

[1] Y. Yang, F. Li, M. Yan, et al. Revealing the toxicity-enhancing essence of Glycyrrhiza on Genkwa flos based on ultra-high-performance liquid chromatography coupled with quadrupole-orbitrap high-resolution mass spectrometry and self-assembled supramolecular technology. Frontiers in Chemistry, 2021, 9: 740952.

[2] L. Martínez, R. Andrade, E. Birgin, et al. A package for building initial configurations for molecular dynamics simulations. Journal of Computational Chemistry, 2009, 30 (13): 2157-2164.

[3] J. Wang, R. Wolf, J. Caldwell, et al. Development and Testing of a General Amber Force Field. Journal of Computational Chemistry 2004, 25 (9): 1157-1174.

[4] M. Abraham, T. Murtola, R. Schulz, et al. GROMACS: High performance molecular simulations through multi-level parallelism from laptops to supercomputers. SoftwareX, 2015, 1: 19-25.

[5] W. Humphrey, A. Dalke, K. Schulten. VMD: visual molecular dynamics. Journal of Molecular Graphics, 1996, 14(1): 33-38.

[6] E. Want, G. O"Maille, C. Smith, et al. Solvent-dependent metabolite distribution, clustering, and protein extraction for serum profiling with mass spectrometry. Analytical chemistry, 2006, 78(3): 743-752.

[7] T. Barri, L. Dragsted. UPLC-ESI-QTOF/MS and multivariate data analysis for blood plasma and serum metabolomics: effect of experimental artefacts and anticoagulant. Analytica Chimica Acta, 2013, 768(1):118-128.

[8] B. Wen, Z. Mei, C. Zeng, et al. metaX: a flexible and comprehensive software for processing metabolomics data. BMC Bioinformatics, 2017, 18: 1-14.